JOURNAL OF AGRICULTURAL AND FOOD CHEMISTRY

Article

pubs.acs.org/JAFC

Metabolism of the Insecticide Metofluthrin in Cabbage (*Brassica oleracea*)

Daisuke Ando,* Masao Fukushima, Takuo Fujisawa, and Toshiyuki Katagi

Environmental Health Science Laboratory, Sumitomo Chemical Company, Ltd., 4-2-1 Takatsukasa, Takarazuka, Hyogo 665-8555, Japan

ABSTRACT: The metabolic fate of metofluthrin [2,3,5,6-tetrafluoro-4-(methoxymethyl)benzyl (*E*,*Z*)-(1*R*,3*R*)-2,2-dimethyl-3-(prop-1-enyl)cyclopropanecarboxylate] separately labeled with ^{14}C at the carbonyl carbon and the α-position of the 4-methoxymethylbenzyl ring was studied in cabbage (*Brassica oleracea*). An acetonitrile solution of ^{14}C-metofluthrin at 431 g ai ha^{-1} was once applied topically to cabbage leaves at head-forming stage, and the plants were grown for up to 14 days. Each isomer of metofluthrin applied onto the leaf surface rapidly volatilized into the air and was scarcely translocated to the untreated portion. On the leaf surface, metofluthrin was primarily degraded through ozonolysis of the propenyl side chain to produce the secondary ozonide, which further decomposed to the corresponding aldehyde and carboxylic acid derivatives. In the leaf tissues, the 1*R*-*trans*-*Z* isomer was mainly metabolized to its dihydrodiol derivative probably via an epoxy intermediate followed by saccharide conjugation in parallel with the ester cleavage, whereas no specific metabolite was dominant for the 1*R*-*trans*-*E* isomer. Isomerization of metofluthrin at the cyclopropyl ring was negligible for both isomers. In this study, the chemical structure of each secondary ozonide derivative was fully elucidated by the various modes of liquid chromatography−mass spectrometry (LC-MS) and nuclear magnetic resonance (NMR) spectroscopy together with cochromatography with the synthetic standard, and their *cis*/*trans* configuration was examined by the nuclear Overhauser effect (NOE) difference NMR spectrum.

KEYWORDS: *metofluthrin, plant metabolism, ozonide, diastereomer*

INTRODUCTION

Metofluthrin (**1**) [SumiOne, Eminence; 2,3,5,6-tetrafluoro-4-(methoxymethyl)benzyl (*E*,*Z*)-(1*R*,3*R*)-2,2-dimethyl-3-(prop-1-enyl)cyclopropanecarboxylate] is a pyrethroid insecticide for household and public hygiene usages developed by Sumitomo Chemical Co., Ltd., and has a strong knockdown activity, especially against mosquitoes. Because of its high volatility (1.96×10^{-3} Pa) with a low mammalian toxicity, **1** can be used in nonheated formulations such as fan-type, paper, and resin emanators.[1] Incidentally, the presence of the two optical centers at the cyclopropenyl ring and one geometrical isomerism at the propenyl side chain result in eight isomers, and **1** consists of the biologically active 1*R*-*trans* isomers having an *E*/*Z* geometrical ratio of 1/8, abbreviated as **1**-*RTE* and **1**-*RTZ*.[1]

The extremely limited emission of **1** to the environment is most likely because it is mainly used indoors. However, as there is no geographic restriction of its use, that is, personal outside insect repellent, **1** may directly or indirectly reach a nontarget environment such as a water body, soil, and plants. In addition, with regard to biocide, submission of relevant data to the European Union and the U.S. Environmental Protection Agency regarding environmental fate has recently become inevitable, irrespective of the use pattern especially due to the possible contamination by sewage treatment plant effluent. From these aspects, it is important to obtain experimental data on **1** to show that it is benign to the environment. The aerobic soil metabolism in two U.S. soils has shown that **1**-*RTZ* and **1**-*RTE* rapidly degrade at similar half-lives of 2.3−3.5 days via cleavage of the ester linkage to produce the corresponding alcohol (**10**) and acid (**7**), followed by successive oxidation at the prop-1-enyl group and the benzyl carbon to form dicarboxylic acid (**11**) and terephthalic acid (**9**) derivatives, respectively.[2] Further degradation of the metabolites resulted in production of carbon dioxide, but little enantiomerization and geometrical isomerization proceeded. Radioactivity was also detected as the soil bound residues. The soil adsorption coefficient (K_{oc}) of **1**-*RTZ* in three German soils was determined to be 3553−6142 mL g^{-1} oc by the batch equilibrium method.[2] Under illumination on the moisture-controlled soil, **1**-*RTZ* degraded with a half-life of 8.1−12.0 days.[3,4] The photodegradation pathway was oxidation of the double bond at the prop-1-enyl moiety and cleavage of the ester linkage, followed by further decomposition to polar compounds and mineralization to carbon dioxide. The major degradates detected were carbonaldehyde (**4**) and carboxylic acid (**5**) derivatives, which were decomposed from ozonide (**2**) and diol (**6**) produced by the activated oxygen species, that is, ozone and hydrogen peroxide, respectively. The photoisomerization hardly proceeded throughout the test duration.[3] In the hydrolysis study, **1**-*RTZ* was moderately degraded by ester cleavage with a half-life of 26.8 days at pH 9 and 25 °C, whereas it was stable at pH 5 and 7. For aqueous photolysis using a xenon arc lamp, **1**-*RTZ* and **1**-*RTE* rapidly dissipated with half-lives of 1.1−3.4 days at pH 7 mainly due to ester cleavage to produce **7** and **10** and oxidation of the olefinic double bond to form **3** and **4**, whereas isomerization was a minor route.[4]

Received: September 26, 2011
Revised: December 21, 2011
Accepted: December 26, 2011
Published: December 26, 2011

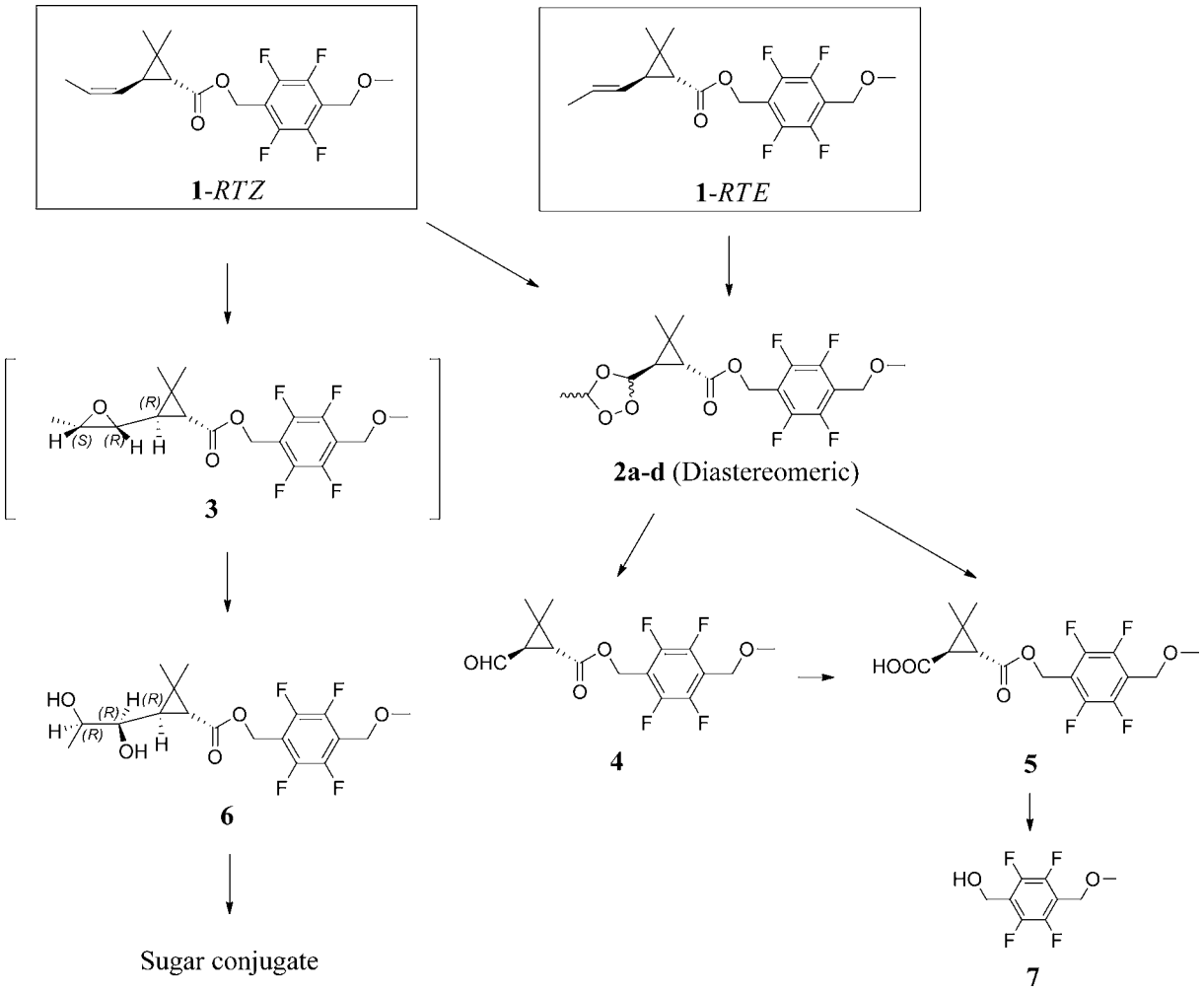

Figure 1. Proposed metabolic pathway of metofluthrin in/on cabbage plant.

Up to this date, the plant metabolism study of **1**, for which information is necessary for the ecotoxicological assessments of nontarget species, is not available. From this standpoint, we have studied the metabolism of **1** in cabbage grown in a greenhouse, which was selected as a model plant because its broad and waxy leaves[5] are considered to be suitable to trap and prevent the loss of **1** by rapid volatilization.[6] The metabolites formed in/on the plant were clarified by extensive spectrometric analysis using LC-MS and NMR spectroscopy in conjunction with direct chromatographic comparison with the synthetic standards.

MATERIALS AND METHODS

Chemicals. The nonradiolabeled metofluthrin (**1**) and its potential degradates as follows were synthesized in our laboratory according to the reported methods.[2−4] The structures of the compounds are referred to Figure 1; 2,3,5,6-tetrafluoro-4-(methoxymethyl)benzyl (1*R*,3*R*)-2,2-dimethyl-3-(3-methyl-1,2,4-trioxolane-5-cyclopropanecarboxylate (**2**); 2,3,5,6-tetrafluoro-4-(methoxymethyl)benzyl (1*R*,3*R*)-2,2-dimethyl-3-(3-methyl-1,2-epoxy)cyclopropanecarboxylate (**3**); 2,3,5,6-tetrafluoro-4-(methoxymethyl)benzyl (1*R*,3*R*)-2,2-dimethyl-3-formylcyclopropanecarboxylate (**4**); 2,3,5,6-tetrafluoro-4-(methoxymethyl)benzyl (1*R*,3*R*)-2,2-dimethyl-3-carboxycyclopropanecarboxylate (**5**); 2,3,5,6-tetrafluoro-4-(methoxymethyl)benzyl (1*R*,3*R*)-2,2-dimethyl-3-(1,2-propanediol)cyclopropanecarboxylate (**6**); 2,3,5,6-tetrafluoro-4-(methoxymethyl)benzyl alcohol (**7**); 2,3,5,6-tetrafluoro-4-(methoxymethyl)benzoic acid (**8**); tetrafluoroterephthalic acid (**9**); (1*R*,3*R*)-2,2-dimethyl-3-(*E*,*Z*)-propenylcyclopropanecarboxylic acid (**10**); (1*R*,3*R*)-2,2-dimethyl-3-carboxycyclopropanecarboxylic acid (**11**). The chemical purity of each standard was determined to be >95% by high-performance liquid chromatography (HPLC). Degradate **2** was prepared according to the following method. Three milligrams of either **1**-*RTZ* or **1**-*RTE* was dissolved in 1 mL of *n*-hexane solution and cooled to < −40 °C using dry ice/acetone prior to the ozone oxidation. Ozone gas produced at an approximate concentration of 20 g $N^{-1}m^{-3}$ using an ozone generator (type 0N-1-2, Nippon Ozone Co., Ltd., Japan) was gently bubbled into the reaction mixture for 3 min at < −40 °C, which resulted in the formation of a white precipitate of crude **2**. After the solution returned to room temperature, **2** was successively purified by HPLC, and the solvent was removed using an evaporator and dried in vacuo to obtain a colorless liquid, the chemical purity of which was determined to be >95%. The chemical structure of **2** was confirmed by various modes of NMR and LC-ESI-MS spectroscopies. **2** was stable in acetonitrile, *n*-hexane, and chloroform for a few months in a freezer below 0 °C, but rapidly decomposed to **4** and **5** in aqueous organic media. The following ^{14}C-labeled isomers of **1** were synthesized in our laboratory with the reported methods;[2−4] **1**-*RTZ* separately labeled at the *α*-position of 2,3,5,6-tetrafluoro-4-methoxymethylbenzyl ring (*benzyl*-^{14}C) or the carbonyl carbon (*carbonyl*-^{14}C) and **1**-*RTE* labled at the carbonyl carbon (*carbonyl*-^{14}C) with specific activities of 0.1654, 0.1651, and 0.1651 mCi mg^{-1}, respectively. *β*-Glucosidase (almond) and cellulase (*Aspergillus niger*) were purchased from Wako Pure Chemical Industries, Ltd. All of the reagents and solvents used were of the analytical grade.

Chromatography. The reversed-phase (RP) HPLC analysis of metabolites within the leaf surface rinse and extract was conducted using a Hitachi LC module (model L-7000) equipped with a SUMIPAX ODS A-212 column (5 μm, 6 mm i.d. × 15 cm, Sumika Chemical Analysis Service (SCAS), Ltd.) at a flow rate of 1 mL min^{-1}. The following gradient system was operated as the typical analysis with acetonitrile containing 0.05% formic acid (solvent A) and distilled water with 0.05% formic acid (solvent B): 0 min, % A/% B, 5/95; 0−3 min, 5/95, isocratic; 3−10 min, 45/55 at 10 min, linear; 10−70 min, 75/25 at 70 min, linear; 70−71 min, 5/95 at 71 min, linear; 71−80 min, 5/95, isocratic (HPLC method 1). For the separation of four isomers of **2**, the gradient system as follows was applied: 0 min, % A (acetonitrile)/% B (water), 53/47; 0−3 min, 53/47, isocratic; 3−43.7 min, 58/42 at 43.7 min, linear; 43.7−44 min, 75/25 at 44 min, linear; 44−51 min, 53/47 at 51 min, linear; 51−60 min, 53/47, isocratic (HPLC method 2). The chiral analysis was conducted with a Shimadzu LC-10AT HPLC system connecting two SUMIPAX DI-NO_2 columns (5 μm, 4 mm i.d. × 25 cm, SCAS) and one CHIRALCEL OD-H column (5 μm, 4.6 mm i.d. × 25 cm, Daicel Chemical Industries, Ltd.) in series using an isocratic eluent of *n*-hexane/ethanol, 1000/0.5 (v/v), at a flow rate of 0.9 mL min^{-1}. The radioactivity eluted was monitored with a Flow Scintillation Analyzer Radiomatic 500TR (Perkin-Elmer Co., Ltd.) or Ramona (Raytest, Germany) radiodetector equipped with a 500 μL liquid cell using Ultima-Flo AP (Perkin-Elmer, Co., Ltd.) as the scintillator. The detection limit of the HPLC analyses was 30 dpm. The typical retention times of **1**-*RTZ* and **1**-*RTE* and their related reference standards have been reported previously.[2−4]

One- or two-dimensional thin-layer chromatography (1D- or 2D-TLC) was carried out for an analytical purpose using precoated silica gel $60F_{254}$ thin-layer chromatoplates (20 × 20 cm, 0.25 mm thickness; E. Merck). The nonradiolabeled reference standards were detected by exposing the chromatoplates to ultraviolet light or spraying bromocresol green reagent for direct visualization. Autoradiograms were prepared by transcribing the TLC plates to BAS-IIIs Fuji imaging plates (Fuji Photo Film Co., Ltd.) for several hours. The radioactivity in each spot exposed onto the imaging plate was detected by a Bio-Imaging Analyzer Typhoon (GE Healthcare). The solvent systems for 2D-TLC were chloroform/methanol, 9/1 (v/v), and toluene/ethyl acetate/acetic acid, 5/7/1 (v/v/v). For the analysis of **2**, *n*-hexane/toluene/acetic acid, 3/15/2 (v/v/v) was applied for 1D-TLC development. The typical R_f values of **1**-*RTZ* and **1**-*RTE* and their related reference standards have been reported previously.[2−4]

Spectroscopy. For NMR spectrometric analyses, one-dimensional (^{1}H, ^{13}C, distorsionless enhancement by polarization transfer (DEPT), nuclear Overhauser effect (NOE) difference) and two-dimensional experiments (^{1}H−^{1}H correlation spectroscopy (COSY), heteronuclear single quantum coherence (HSQC), heteronuclear multiple-bond connectivity (HMBC), NOE correlated spectroscopy (NOESY)) were employed in *d*-chloroform including tetramethylsilane (TMS) using a Varian Mercury 400 (Varian Technologies Ltd.) spectrometer (400 MHz).

Liquid chromatography−electrospray ionization−mass spectrometry (LC-ESI-MS) analysis was conducted using a Waters Micromass ZQ spectrometer equipped with a Waters separation module 2695 and photo array detector 2996 as a liquid chromatograph. For the conventional analysis of metabolites, HPLC method 1 was applied with the analytical parameters controlled by MassLynx software (version 4.00) as shown: source temperature, 100 °C; desolvation temperature, 350 °C; capillary voltage, 3.2 kV; cone voltage, 10−40 V. For the analysis of **2**, conditions of source temperature, 70 °C, and desolvation temperature, 300 °C, were selected to mitigate its thermal degradation and the gradient system as follows was applied: 0 min, % A (acetonitrile)/% B (methanol/20 mM ammonium acetate (20/10, v/v))/% C (water), 5/30/65; 0−50 min, 20/30/50, linear.

Radioanalysis. Radioactivity in the liquid surface rinse and extract from plant was determined by mixing each aliquot with 10 mL of Packard Emulsifier Scintillator Plus and analyzed by liquid scintillation counting (LSC) with a Packard model 2900TR spectrometer. The background level of radioactivity in LSC was 30 dpm, which was subtracted from the dpm value of a measured sample. The ^{14}C in the extracted residues and untreated plant portions was converged and measured as $^{14}CO_2$ using a Packard model 307 sample oxidizer. $^{14}CO_2$ produced was absorbed into 9 mL of Packard Carb-CO_2 absorber and mixed with 15 mL of Packard Permafluor scintillator, and the radioactivity therein was quantified by LSC. The efficiency of combustion was determined to be >95.8%.

Plant Material and Treatment. Cabbage (*Brassica oleracea* var. *capitata*, cv. Green Ball) was grown in a 1/5000-are Wagner pot filled with Kasai soil (Hyogo, Japan) in a greenhouse at 25 °C during the day and at 20 °C during the night. The application of each [^{14}C] -**1** to the cabbage plants was conducted at the plant growth stage of BBCH 41.[7] The average surface area and weight of a cabbage leaf at the application stage were 176.6 cm^2 and 10.31 g, respectively. The characterization of Kasai soil is as described as follows: soil texture (%), sand 82.9, silt 8.9, clay 8.2; soil classification, sandy loam; organic carbon content (w/w), 1.7; pH (H_2O), 6.6; maximum water-holding capacity (g per 100 g of dry soil), 28.19.

The application dose of **1** to cabbage plants was 431 g ai ha^{-1}, which was determined by assuming that a typical commercial can was directly sprayed onto cabbage leaves as the worst-case scenario: 4 g of aerosol of the water-based formulation containing 0.1% (w/w) of **1** was sprayed once onto a square-foot field for the purpose of general insect repellent. Although the isomeric ratio of **1**-*RTZ* and **1**-*RTE* in the active ingredient is 8/1, the same dosing rate was used for each isomer in this study. For the leaf treatment, the dosing solution per leaf was prepared by mixing 0.167 MBq of each [^{14}C]-**1** isomer with 0.761 mg of the corresponding unlabeled material in 100 μL of acetonitrile (0.212 MBq mg^{-1}). The prepared dosing solution was topically applied onto nine leaves (three leaves × three pots) using a microsyringe for each label. With respect to the soil treatment, the dosing solution per pot was prepared by combining 1.667 MBq of each [^{14}C]-**1** with 0.862 mg of the unlabeled material in 1 mL of acetonitrile and was applied onto 120 g of Kasai soil in a plastic bag using a pipet and thoroughly mixed for 30 min. After evaporation of acetonitrile, it was gently put onto the soil surface of the Wagner pot in which cabbage plants were grown.

Sampling, Extraction, and Analysis. For leaf treatment, three cabbage leaves per pot were harvested at 2, 7, and 14 days after treatment. The leaves were individually cut from the stem using scissors, and untreated leaves and stems were similarly sampled with another uncontaminated one. For soil treatment, both cabbage plant and soil were separately sampled at 14 days after treatment. The whole cabbage plant was obtained by cutting the stem just above the ground. The dried soil was vertically divided into three layers according to its depth (top, 0−2 cm; middle, 2−10 cm; bottom, 10−18 cm), and the root was removed from the soil. All samples were immediately weighed and stored in a freezer (below −20 °C) until analysis.

In the case of the leaf treatment, the surface of treated leaves was rinsed with 100 mL of methanol per leaf. The rinsed leaf was cut into small pieces and homogenized with 20 mL of methanol at 10000 rpm and 0 °C for 10 min using a homogenizer AM-8 (Nissei Ltd., Japan). The homogenate was vacuum filtered to separate the extract and the residue. The residue remaining after filtering was extracted again in the same manner, and the filtrate was combined. The process was repeated using methanol/water (4/1, v/v). Each aliquot of the surface rinse, methanol, and methanol/water extracts was analyzed with LSC, HPLC, and 2D-TLC. The extracted residues were air-dried and individually combusted for LSC analysis. For the soil treatment, a portion of each soil layer was subjected to a combustion analysis to determine the residual amount of ^{14}C. Approximately 50 g of the evenly mixed top layer soil for each label was transferred into 200 mL plastic centrifuge bottles, and 100 mL of methanol was added. The bottle was mechanically shaken for 10 min with a Taiyo SR-IIw recipro-shaker and then centrifuged at 5000 rpm at 4 °C for 10 min using a himac CR20G high-speed refrigerated centrifuge (Hitachi Ltd., Japan). The extract was recovered from the bottle by decantation, the residues were repeatedly extracted twice in the same manner, and then the extracts were combined. The procedure was repeated using methanol/concentrated HCl (100/1, v/v). After radioassay by LSC,

Table 1. Distribution of Radioactivity after Foliar Applications

	% of the applied radioactivity					
	[benzyl-^{14}C] **1**-*RTZ*		[carbonyl-^{14}C] **1**-*RTZ*		[carbonyl-^{14}C] **1**-*RTE*	
	2 D	14 D	2 D	14 D	2 D	14 D
Surface	65.6	11.8	50.1	26.3	61.7	15.8
Extract						
Methanol	7.4	17.1	27.2	39.2	17.5	32.9
75%Methanol	1.0	0.9	3.5	3.0	0.6	2.5
Unextractable	0.5	1.6	0.6	2.6	2.1	3.1
Untreated plant	N.D.[a]	N.D.	N.D.	N.D.	N.D.	N.D.
Untreated soil	N.D.	N.D.	N.D.	N.D.	N.D.	N.D.
Total	74.5	31.4	81.4	71.1	81.9	54.3

[a]nd, not detected.

Table 2. Distribution of 1 and Its Metabolites in Treated Cabbage Leaves

	% of the total radioactive residue								
	[benzyl-^{14}C] **1**-*RTZ*			[carbonyl-^{14}C] **1**-*RTZ*			[carbonyl-^{14}C] **1**-*RTE*		
	2 D	7 D	14 D	2 D	7 D	14 D	2 D	7 D	14 D
Surface rinse									
1-*RTZ*	45.0	6.8	N.D.[a]	7.8	0.5	N.D.	N.D.	N.D.	N.D.
1-*RTE*	N.D.	N.D.	N.D.	N.D.	N.D.	N.D.	59.6	1.5	N.D.
2a	6.6	10.0	N.D.	2.3	9.1	2.1	1.7	6.9	3.0
2b	3.5	5.2	N.D.	1.4	5.3	2.0	1.0	4.2	1.7
2c and **2d**	5.8	10.2	N.D.	2.3	7.9	3.6	1.5	3.2	2.1
4	21.3	12.0	6.6	28.5	11.3	2.5	9.7	21.9	4.6
5	2.9	13.3	26.0	12.8	17.5	14.1	1.8	13.6	14.7
Others[b]	3.0	9.2	5.0	6.5	3.5	12.7	N.D.	4.9	3.1
Subtotal	88.1	66.7	37.6	61.6	55.1	37.0	75.3	56.2	29.2
Extract									
1-*RTZ*	1.0	0.4	8.5	15.7	18.6	1.5	N.D.	N.D.	N.D.
1-*RTE*	N.D.	N.D.	N.D.	N.D.	N.D.	N.D.	18.5	11.6	9.4
4	0.2	1.4	N.D.	2.4	1.0	N.D.	0.3	0.5	4.0
5	N.D.	N.D.	1.4	N.D.	N.D.	N.D.	N.D.	1.7	4.6
6 conjugate[c]	3.1	3.7	11.3	7.2	6.6	12.3	N.D.	N.D.	N.D.
7	0.5	8.7	12.2	-[d]	-	-	-	-	-
Others[e]	6.4	15.1	23.4	12.4	18.0	45.5	3.3	22.2	47.2
Subtotal	11.2	29.3	57.3	37.7	44.2	59.3	22.1	37.0	65.2
Total	100.0	100.0	100.0	100.0	100.0	100.0	100.0	100.0	100.0

[a]nd, not detected; [b]Consisted of multiple components, each of which amounted to <2.0%. [c]Sugar conjugate of **6**. [d]–, not available. [e]Consisted of multiple components, each of which amounted to <7.0%.

the extracts were concentrated using an evaporator, and each 10000 dpm was subjected to HPLC and 2D-TLC analyses. The soil residues after extraction were air-dried in open vessels at room temperature for several days and subjected to combustion analysis to determine the remaining radioactivity.

The total radioactive residue (TRR) in the test system of the foliar application was determined as the sum of ^{14}C in the surface rinse, extract and unextractable. The TRR recovered from the test system of the soil treatment was determined as the sum of ^{14}C in extractable and unextractable fractions of topsoil and that in the middle and bottom soil layers and plant.

Identification of Metabolites. In general, the identity of the metabolites was confirmed by HPLC and 2D-TLC cochromatographies with the nonradiolabeled reference standards. In addition, LC-ESI-MS and NMR analyses were carried out for identification of **2**. To identify conjugated metabolites, approximately 200 000 dpm of the extract was dissolved in 1 mL of 10 mM sodium acetate buffer at pH 5.0, and 10 mg of cellulase or β-glucosidase was added to the solution. The mixture was incubated in a BR-180LF BioShaker (TAITEC Co. Ltd., Japan) at 37 °C and 100 rpm. The aliquot of the reaction mixture was sampled sequentially until 7 days after incubation and directly analyzed with HPLC and 2D-TLC. With regard to the characterization of metabolites in the extract, chemical derivatizations (acetylation and methylation) were performed. The leaf extracts including 100 000 dpm were taken and the solvent was dried up using an evaporator. The dried extract was redissolved in 500 μL of pyridine/acetic anhydride (50/50, v/v) and allowed to stand overnight for acetylation and then dissolved again in 500 μL of acetonitrile with dropwise addition of 20 μL of 0.1% trimethylsilyldiazomethane in *n*-hexane and mixing for 4 min for methylation. The derivatized samples were directly analyzed by HPLC.

For the purpose of collecting a sufficient amount of **2** for LC-MS and NMR analyses, 0.167 MBq of [*benzyl*-^{14}C]-**1**-*RTZ* mixed with 10 mg of the nonradiolabeled material in acetonitrile was applied onto the surface of three cabbage leaves. The plants were grown in the greenhouse for 7 days. After the sampling, the treated leaves were rinsed with acetonitrile and the rinsate was subjected to isolation of **2** using HPLC method 2.

RESULTS

Distribution of ^{14}C in Plant and Soil. The distribution of radioactivity after the foliar application is summarized in Table 1. For the leaf treatment, the radioactivity recovered from the treated leaves was 31.4–71.1% of the applied radioactivity (% AR) after 14 days. The unrecovered ^{14}C was most likely lost by vaporization, considering the vapor pressure (1.96×10^{-3} Pa) and Henry's law constant (2.1×10^{-4} m^3 mol^{-1}) of **1**. The ^{14}C recovered by the surface rinse gradually decreased to 11.8–26.3%AR at the end of the study, whereas that in the leaf extract concomitantly increased to 18.0–42.2%AR. The total

dx.doi.org/10.1021/jf203903r | J. Agric. Food Chem. 2012, 60, 2607–2616

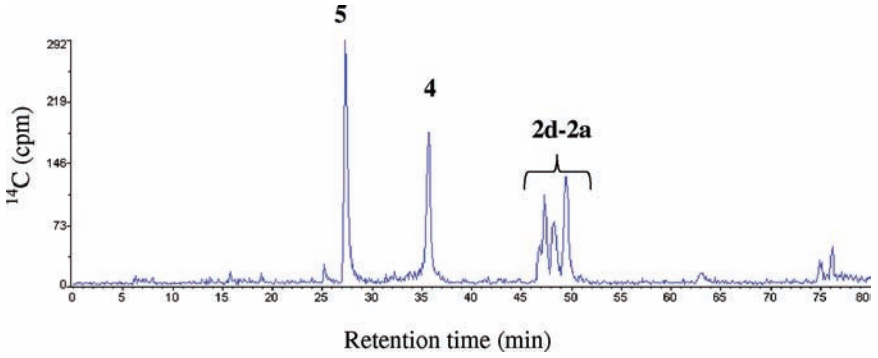

Figure 2. RP-HPLC chromatogram of the surface rinse of [*carbonyl*-^{14}C]-**1**-*RTZ* treated leaf after 7 days. Numbers above each peak indicate the corresponding metabolite.

amount of unextractable ^{14}C was <3.1%AR during the study in any case. Little radioactivity was translocated from the treated leaf to the untreated portions of plant. With respect to the soil treatment, ^{14}C recovered from the test system was 39.6−60.4% AR after 14 days. The majority of the radioactivity remained in the top layer of soil (0−2 cm), which amounted to 12.1−30.9% AR, whereas levels in the middle (2−10 cm) and bottom (10−18 cm) layers of soil were 13.1−16.1 and 4.8−9.9%AR, respectively. The uptake of ^{14}C from the soil to the plant was negligible at 1.5−3.6%AR.

The metabolite distribution for the leaf treatments is summarized in Table 2. The representative HPLC chromatogram of the surface rinse fraction is shown in Figure 2. On the leaf surface, **1**-*RTZ* and **1**-*RTE* were rapidly dissipated to <0.1% of the total radioactive residue (%TRR) at 14 days after treatment. **2**, **4**, and **5** were detected as major metabolites, with maximum amounts reaching 25.4, 28.5, and 26.0%TRR, respectively, at 7 days after treatment. In addition, **2** was clearly separated into four peaks by using HPLC method 2; that is, the retention times of **2a**, **2b**, **2c**, and **2d** were 33.7, 31.7, 30.0, and 29.3 min, respectively, which indicated the presence of four isomers. Other minor metabolites were <2.0%TRR. In the leaf extract, **1**-*RTZ* and **1**-*RTE* were detected at 0.4−18.6 and 9.4−18.5%TRR, respectively, during the test duration. Comparison of the metabolic profile has shown that it is relatively different between **1**-*RTZ* and **1**-*RTE*. In the case of **1**-*RTZ*, the major metabolite having an intact ester linkage was the glucose conjugate of **6**, amounting to its maximum 12.3% TRR. **7** was detected at 12.2%TRR for the benzyl label, but no corresponding degradates unique to the cyclopropane label exceeding 10%TRR were observed, which suggested faster degradation for the acid moiety in the cabbage plant. For **1**-*RTE*, **4** and **5** were formed at 4.0 and 4.6%TRR, respectively, and none of the metabolites exceeded 7%TRR. To evaluate the isomerization ratio, the chiral HPLC analysis of **1**-*RTZ* and **1**-*RTE* remaining on/in the leaf for the benzyl label was conducted, which demonstrated negligible isomerization to the other stereoisomers (<0.7%TRR). For the soil treatment, most of the radioactivity remained as the intact parent compound except for [*benzyl*-^{14}C] **1**-*RTZ*, which produced **8** in 41.9%TRR at 14 days after treatment.

Identification of Metabolite 2. Approximately 180 and 250 ng of isomeric metabolites **2a** and **2b** were obtained, respectively, from the experiment on collecting sufficient amounts for their identification. The purified metabolites **2a** and **2b** were individually subjected to ^{1}H NMR and ^{1}H−^{1}H COSY and 1D- and 2D-TLC analyses. The chemical shifts of these metabolites are listed in Table 3. Each proton signal pattern was very similar between the two isomers, but was clearly different from that of **1**-*RTZ* as its two methine protons at the propenyl moiety shifted from 4.92 and 5.35 ppm to a lower magnetic field of 5.11 and 5.62 ppm, respectively. With regard to the ^{1}H−^{1}H COSY spectrum, no cross signal was observed between the above two adjacent methine protons for **2a** and **2b**, which suggested the cleavage of the C−C double bond (Figure 3). In the 1D-TLC analysis using an acidic solvent C, both **2a** and **2b** decomposed to carbonaldehyde (**4**) and carboxylic acid (**5**) derivatives during the development. Therefore, the chemical structures of **2a** and **2b** were assumed to be ozonide derivatives possessing a 1,2,4-trioxolane ring. To definitively identify the chemical structure of ozonide, **2** was synthesized from **1**-*RTZ* and **1**-*RTE*. The modification of HPLC gradient system (method 2) enabled the synthetic **2** to be separated into four isomers, namely, **2a**−**2d**. The observed ratio of the four isomers was **2a**/**2b**/**2c**/**2d** = 33/16/37/14 for **1**-*RTZ* and **2a**/**2b**/**2c**/**2d** = 40/21/28/11 for **1**-*RTE*. The ^{1}H and ^{13}C NMR spectra of each isomer are listed in Table 3. The overall trends of the spectra were similar within four isomers, but the chemical shifts related to protons H5 and H6 on the cyclopropane ring were clearly different. The four isomers all exhibited identical cross peaks in various modes of 2D-NMR analyses, which clearly demonstrated the preservation of the chemical structures of the parent compound except for the cleavage of the C−C double bond at the prop-1-enyl moiety. In the LC-ESI-MS analysis, the pseudo ions of **2a**−**2d** were observed at *m*/*z* 409 $[M + H]^+$, 426 $[M + NH_4]^+$, and 431 $[M + Na]^+$ in the positive ion mode, which indicated the addition of three oxygen atoms to **1**. Taking all of the above into account, these four products were determined to be the diastereomers of the ozonide derivative, for which the two asymmetric carbons exist in the trioxolane ring. Incidentally, by comparison of the ^{1}H and ^{1}H−^{1}H NMR spectra and TLC, the HPLC cochromatogram has clarified that **2a**−**2d** produced on the leaf surface were identical with those of the synthesized standards. In addition, the HPLC-purified synthetic isomers **2a**, **2b**, and the mixture of **2c** and **2d** were subjected to NOE difference analysis to obtain steric information. The NOE resonance was clearly observed between the protons H10 (5.34−5.36 ppm) and H11 (4.92−4.96 ppm) in the trioxolane ring for the mixture (**2c** + **2d**), whereas scarce or no resonance was observed for **2a** and **2b**, which indicated the structural distance between these protons is closer for the former isomers compared to the latter (Figure 4), thus characterizing their configurations as *trans* (*threo*) and *cis* (*erythro*), respectively.

Table 3. ^{1}H and ^{13}C NMR Chemical Shifts of 2 Isomers (2a−2d) in *d*-Chloroform

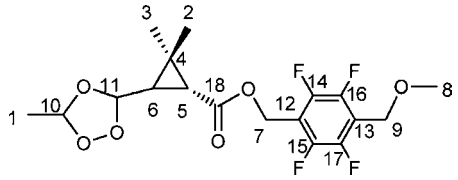

Isomer	Atom	^{1}H (ppm)	^{13}C (ppm)
	1	1.43 (3H, d, J = 4.81 Hz, -C$\underline{H}_3$)	16.18
	2	1.23 (3H, s, -C$\underline{H}_3$)	20.45
	3	1.24 (3H, s, -C$\underline{H}_3$)	21.95
2a	4	-[a]	26.81
	5	1.75 (1H, d, J = 5.61 Hz, cyclopropane-1)	30.49
	6	1.67 (1H, dd, J = 5.21, 7.21 Hz, cycloplopane-3)	31.56
	10	5.35 (1H, q, J = 4.81 Hz, trioxolane-3)	101.81
	11	4.92 (1H, d, J = 7.21 Hz, trioxolane-5)	104.16
	1	1.43 (3H, d, J = 4.80 Hz, -C$\underline{H}_3$)	16.42
	2	1.26 (3H, s, -C$\underline{H}_3$)	20.52
	3	1.27 (3H, s, -C$\underline{H}_3$)	21.82
2b	4	-	26.61
	5	1.69 (1H, d, J = 5.61 Hz, cyclopropane-1)	30.26
	6	1.65 (1H, dd, J = 5.61, 7.21 Hz, cyclopropane-3)	31.00
	10	5.36 (1H, q, J = 4.80 Hz, trioxolane-3)	102.03
	11	4.93 (1H, d, J = 7.21 Hz, trioxolane-5)	103.92
2c **2d**	1	1.46 (3H, d, J = 4.81 Hz, -C$\underline{H}_3$) 1.46 (3H, d, J = 4.81 Hz, -C$\underline{H}_3$)	18.03, 18.24
2c **2d**	2	1.23 (3H, s, -C$\underline{H}_3$) 1.25 (3H, s, -C$\underline{H}_3$)	20.45, 20.52
2c **2d**	3	1.24 (3H, s, -C$\underline{H}_3$) 1.26 (3H, s, -C$\underline{H}_3$)	21.95
2c **2d**	4	- -	26.77, 26.91
2c **2d**	5	1.71 (1H, d, J = 5.21 Hz, cyclopropane-1) 1.66 (1H, d, J = 5.21 Hz, cyclopropane-1)	31.00, 31.56
2c **2d**	6	1.74 (1H, dd, J = 5.21, 7.21 Hz, cyclopropane-3) 1.72 (1H, dd, J = 5.21, 7.21 Hz, cyclopropane-3)	33.58, 33.71
2c **2d**	10	5.34 (1H, q, J = 4.81 Hz, trioxolane-3) 5.34 (1H, q, J = 4.81 Hz, trioxolane-3)	101.86, 101.90
2c **2d**	11	4.96 (1H, d, J = 7.21 Hz, trioxolane-5) 4.96 (1H, d, J = 7.21 Hz, trioxolane-5)	103.78, 103.81
	7	5.24 (2H, s, benzyl)	54.02
	8	3.41 (3H, s, -OC$\underline{H}_3$)	58.75
	9	5.24 (2H, s, benzyl)	61.62
2a-2d[b]	12	-	114.78
	13	-	117.17
	14, 15	-	144.12
	16, 17	-	146.48
	18	-	170.51

[a]−, not available. [b]All of the isomers **2a−2d** showed identical chemical shifts for ^{1}H and ^{13}C NMR.

Identification of Metabolites 3−7. The chemical structures of **3**−**5** and **7** were confirmed by HPLC and 2D-TLC cochromoatographies with the synthetic standards. For the glucose conjugate of **6**, the corresponding HPLC fraction was isolated and then incubated with cellulase or β-glucosidase. A new peak produced by the enzymatic hydrolysis was identified as **6** by the HPLC and 2D-TLC cochromatographies with the reference standard. Interestingly, the enzymatically liberated aglycone **6** predominantly consisted from the single isomer observed at the retention time of 20.9 min, the reference standard of which has four isomers in total.

DISCUSSION

Significant loss of the radiocarbon, that is, maximum 25.6%AR within 2 days, was observed after the foliar application of **1**-*RTZ* and **1**-*RTE* onto the cabbage plant (Table 1), which indicated their immediate volatilization from the leaf surface due to the high vapor pressure. The volatilization of pesticides from leaf surfaces can be conveniently evaluated with Henry's law constant. A similar trend in volatility as for **1** (2.1×10^{-4} m^3 mol^{-1}) was observed for other pyrethroids possessing a high Henry's law constant such as fenpropathrin (1.8×10^{-4} m^3 mol^{-1}), phenothrin (1.4×10^{-6} m^3 mol^{-1}), permethrin ($1.9 \times$

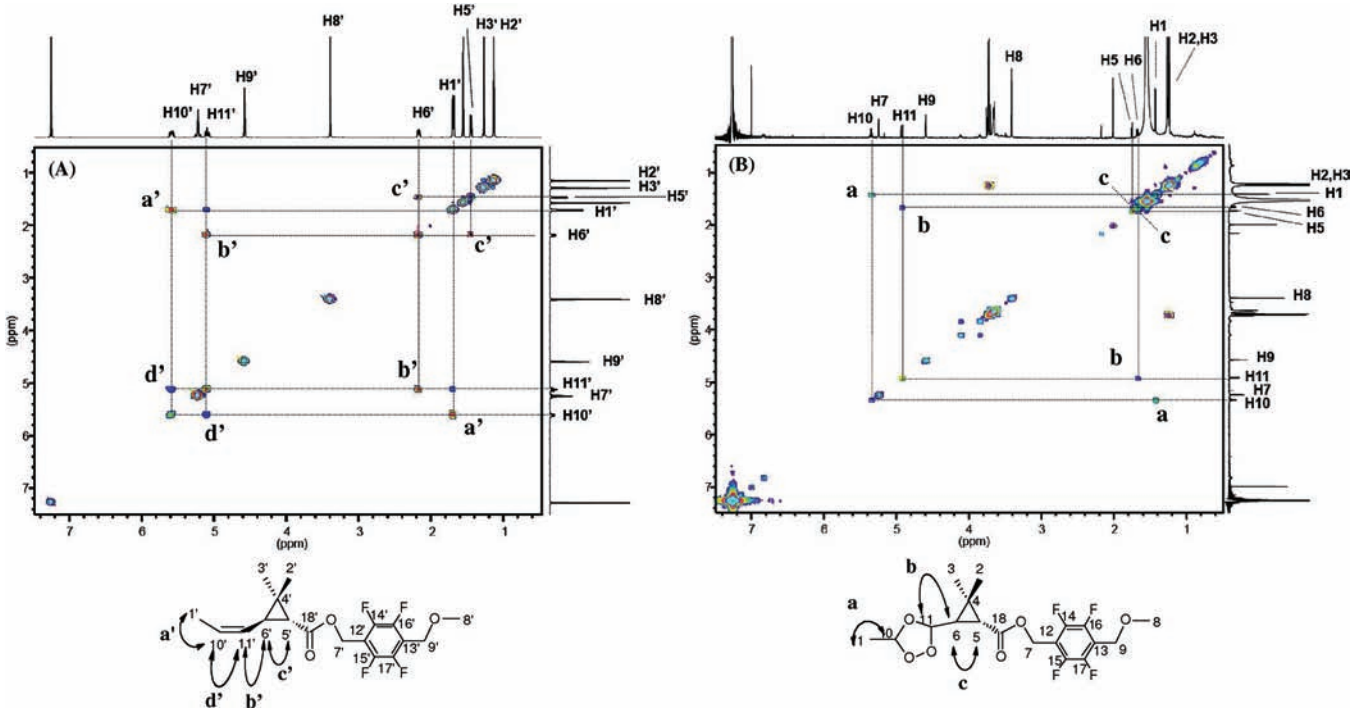

Figure 3. $^{1}H-^{1}H$ COSY spectra of **2a** and **1**-*RTZ* in *d*-chloroform (273 K): (A) spectrum of **1**-*RTZ*; (B) spectrum of metabolite **2a**.

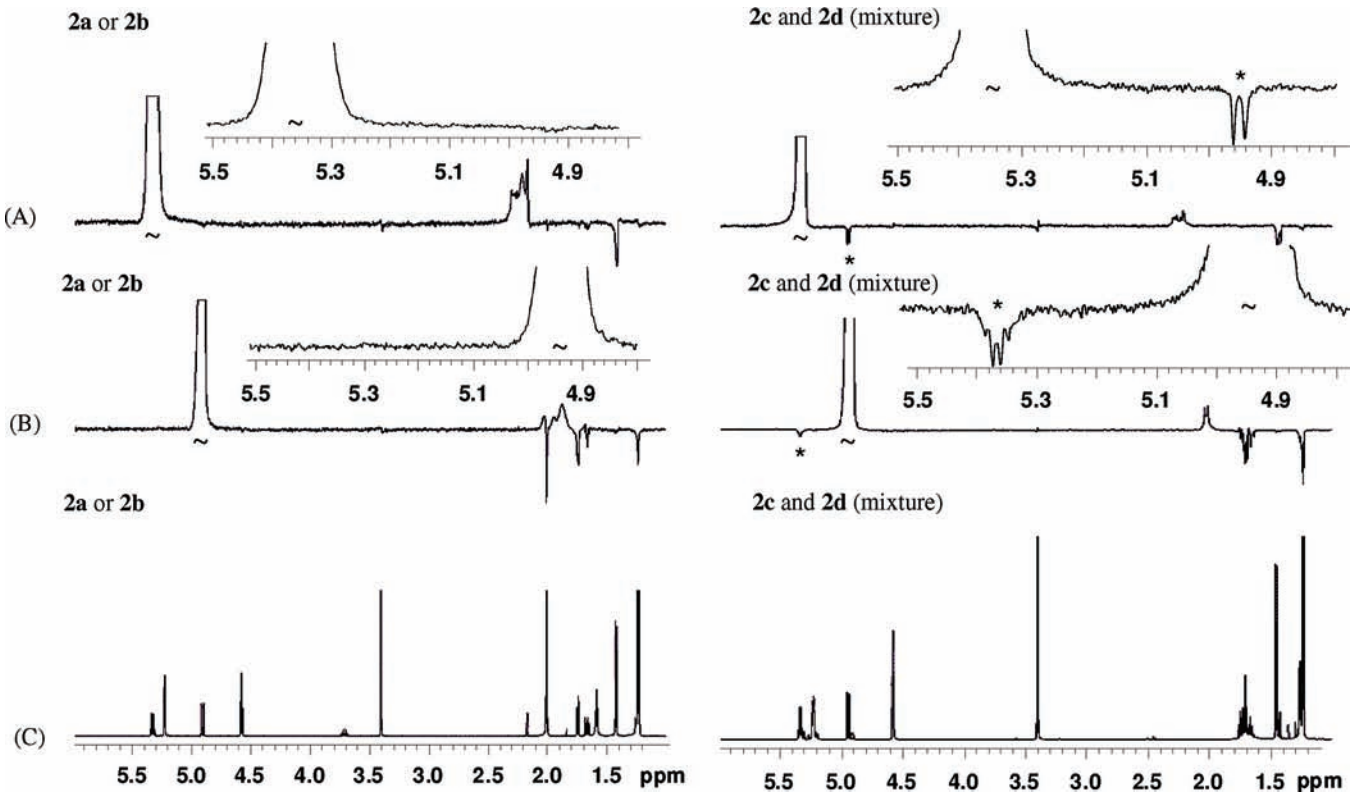

Figure 4. 1D-NOE spectra of **2** isomers in *d*-chloroform (273 K). (A, B) 1D-NOE spectra (5000 scans, delay = 5.0 s, τ_m = 0.375 s, LB = 0.5 Hz) of **2a** or **2b** (left) and mixture of **2c** and **2d** (right) after selective irradiation of proton at the ozonide ring. The irradiation targets are indicated by a tilde (~). The characteristic NOE response between the protons at the ozonide ring was observed only for the mixture of **2c** and **2d** by simultaneous irradiation of the proton signals at the ozonide ring (signals marked by an asterisk). (C) Conventional ^{1}H spectrum (16 scans) of **2a** or **2b** (left) and mixture of **2c** and **2d** (right).

10^{-6} m^3 mol^{-1}), and cypermethrin (4.2×10^{-7} m^3 mol^{-1}), whereas those with a low hHenry's law constant tend to remain on the leaf surface for a relatively longer period, such as tralomethrin (3.9×10^{-15} m^3 mol^{-1}).[8−13]

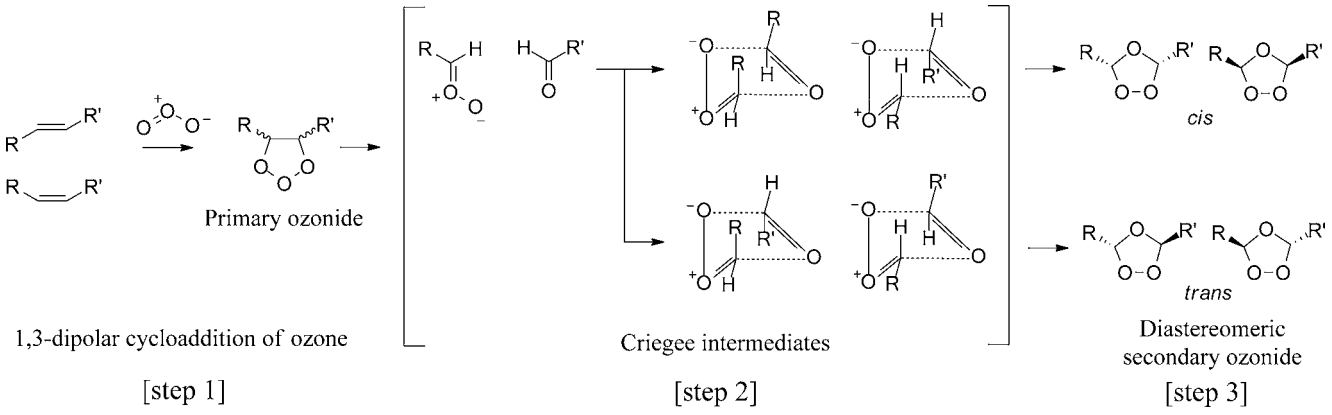

Figure 5. Scheme of diastereomeric secondary ozonide production via the Criegee intermediate.

Both *E*/*Z* geometrical isomers reacted with atmospheric O_3 on the leaf surface to form diastereomeric **2** as the major initial degradates. There are many examples indicating the possible formation of ozonide formation as a degradation intermediate of pyrethroids, but the detection of ozonide is limited due to their instability. Ruzo et al. studied the ozonolysis of synthetic pyrethroids, phenothrin and halothrin, in several organic solvents or on thin films and detected their ozonide derivatives, which were tentatively identified by chemical ionization−mass spectrometry (CI-MS) and ^{19}F, ^{13}C, and ^{1}H NMR spectroscopy.[14] Nambu et al. studied the metabolism of phenothrin on bean foliage and identified its ozonide form by measuring its molecular weight with electron ionization−mass spectrometry (EI-MS) and detecting its typical degradates produced, such as the carbonaldehyde and carboxylic acid derivative during the 1D-TLC development using an acidic solvent.[8] Incidentally, the halogen-substituted pyrethroids, for example, deltamethrin, form lesser amounts of ozonide products[14] and corresponding degradates in the plant metabolism.[9−11] Substituent groups at olefins are considered to be an important factor to determine the reactivity with ozone because an electron-withdrawing substituent reduces the electron density of the olefin, which suppresses the 1,3-dipolar cycloaddition of ozone, whereas an electron-donating group enhances it.[15] Because **2** has two asymmetric carbons at the 1,2,4-trioxolane ring, there are four diastereomers **2a**−**2d** that could be separated by using HPLC method 2. The synthetic reference **2** was confirmed to be identical with those generated from **1**-*RTZ* and **1**-*RTE* on the leaf surface of cabbage plant, and the isomeric ratio was also similar between them. From the detailed analysis of the exclusive data obtained from the 1D-NOE measurement together with the spectrum pattern and chemical shifts/coupling constants of various NMR analyses, the diastereomeric configurations of **2** isomers were determined as *trans* (*threo*) for **2a** and **2b** and *cis* (*erythro*) for **2c** and **2d**. In the ^{13}C NMR spectra, the chemical shifts of C1 and C6 attached to the ozonide ring shifted to lower field and C11 shifted to higher field for **2a** and **2b** compared to those of **2c** and **2d**. This difference in the chemical shifts was in good agreement with the results reported by Griesbaum et al.,[16] who conducted extensive analyses to determine the configuration of the several ozonide derivatives by ^{13}C NMR analysis. Furthermore, **2a** and **2b** were more likely to be produced from **1**-*RTE*, whereas **2c** and **2d** were formed from **1**-*RTZ* by ozonolysis. This result supports our diastereomeric assignment; the empirical trend in selectivity, which has been theoretically examined, especially for bulky substituents, is that *trans* alkenes are more likely to be transformed to *trans* secondary ozonide via *trans* primary ozonide and *syn* carbonyl oxide, and *cis* alkenes, vice versa.[15,17−19] The production of four diastereomers in the ozonolysis of olefins can be explained from a generalized observation on the "Criegee intermediate",[17−22] as summarized in Figure 5, which can be briefly expressed by three steps: (1) 1,3-dipolar cycloaddition of O_3 to olefin to produce a highly unstable primary ozonide, (2) dissociation of the primary ozonide to give the corresponding zwitterionic carbonyl oxide and carbonyl compounds, that is, the Criegee intermediate, and (3) recombination of the Criegee intermediate via another 1,3-dipolar cycloaddition to produce more stable secondary ozonide. Step 2 is considered to be a very important reaction to produce four diastereomers on the cabbage leaf surface, in which the four patterns of nonhomologous random recombination of carbonyl oxide ions and carbonyl compounds produced from the primary ozonide may be deeply involved. Incidentally, the secondary ozonides are considered to be less toxic to mammals because they are highly likely to be unstable in mammalian tissue due to their rapid decomposition in aqueous solutions.[23−25] Furthermore, an ozonide derivative of unsaturated lipid, methyl oleate, was orally administered to rats, which resulted in low toxicity, probably due to its fast degradation by enzymes and biological antioxidants such as glutathione transferase and vitamins, respectively.[25]

In the leaf tissue, the sugar conjugate of **6** was produced as a major metabolite only in leaves treated with **1**-*RTZ*. This may be explained by the selective epoxidation of **1**-*RTZ* to produce intermediate **3** under the function of enzymes probably by cytochrome P450 (CYP), because CYP-catalyzed stereoselective epoxidation of olefins is a common reaction in living organisms such as lipid/hormone biosynthesis and xenobiotic detoxification.[26−29] Although **3** was detected from neither **1**-*RTZ* nor **1**-*RTE* in cabbage plant, the epoxide derivative of **1** is reported to be produced in rat and via photodegradation on soil.[3,30] Vaz et al. clarified that the epoxidation of olefins with the CYPs from several origins proceeded more favorably with (*Z*)-2-butene than its (*E*)-isomer.[28] Sauveplane et al. reported the CYP derived from *Arabidopsis* (*Arabidopsis thaliana*), which was heterologously expressed in yeast (*Saccharomyces cerevisiae*), showed highly selective conversion of (*Z*)-configured unsaturated fatty acids to mono- or di-*cis*-epoxide.[29] Incidentally, Ando et al. extensively studied the configuration of the epoxy chrysanthemate derivatives of (*S*)-bioallethrin and phenothrin produced by mouse microsomal CYP.[31−33] They

have clarified that the oxygen atom was inserted into the propenyl double bond from the *si* face to produce the 7,8-epoxy derivative and its configuration at C7 carbon, the one adjacent to the cyclopropane ring, was *R* and *S* from selective oxidation of *trans*- and *cis*-chrysanthemates, respectively. Additionally, epoxy hydrolases, which transform epoxy derivatives into diols, are also reported to be stereoselective. Soybean-derived epoxy hydrolase converts *cis*-epoxy fatty acids into *threo* diols by catalyzing *trans* addition of water into oxirane carbon, which has the *S*-chirality.[34] Taking all above into consideration, a single isomer of aglycone **6** detected in the cabbage plant is most likely to be the *threo* isomer in *R*−*R* configuration, which was produced via the intermediate *cis* isomer of **3** in *R*−*S* configuration, as its estimated pathway is proposed in Figure 6.

In summary, the proposed metabolic pathway of **1** in the cabbage plant is described in Figure 1. 1-*RTZ* and **1**-*RTE*

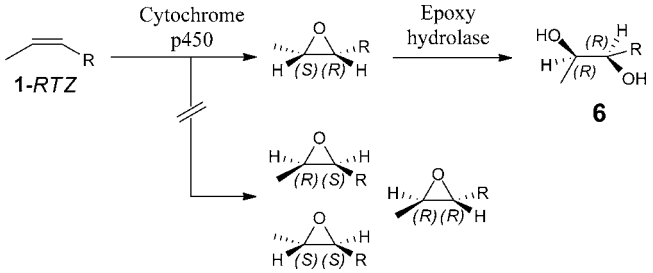

Figure 6. Proposed enzymatic dihydroxylation pathway of **1**-*RTZ*.

reacted with atomospheric O_3 on the leaf surface to form ozonide as the initial product and successively decomposed to carbonaldehyde and carboxylic acid derivatives via opening of the trioxolane ring. In the leaf cell, they were further converted to the polar metabolites via cleavage of the ester linkage and dihydroxylation at the olefinic carbon followed by conjugation with sugar. The isomerization on/in the cabbage leaf was a minor reaction.

AUTHOR INFORMATION

Corresponding Author

*E-mail: andod@sc.sumitomo-chem.co.jp.

REFERENCES

(1) Matsuo, N.; Ujihara, K.; Shono, Y.; Iwasaki, T.; Sugano, M.; Yoshiyama, T.; Uwagawa, S. Discovery and development of a novel pyrethroid insecticide 'Metofluthrin (SumiOne®, Eminence®)'. *Sumitomo Kagaku II* **2005**, 1−15.

(2) Kodaka, R.; Suzuki, Y.; Sugano, T.; Katagi, T. Aerobic metabolism and adsorption of pyrethroid insecticide metofluthrin in soil. *J. Pestic. Sci.* **2007**, *32*, 393−401.

(3) Nishimura, H.; Suzuki, Y.; Nishiyama, M.; Fujisawa, T.; Katagi, T. Photodegradation of insecticide metofluthrin on soil, clay minerals and glass surface. *J. Pestic. Sci.* **2011**, *36*, 376−38.

(4) Nishiyama, M.; Suzuki, Y.; Katagi, T. Hydrolysis and photolysis of insecticide metofluthrin in water. *J. Pestic. Sci.* **2010**, *35*, 447−455.

(5) Baker, E. A. Chemistry and morphology of plant epicuticular waxes. In *The Plant Cuticle*; Cutler, D. F., Alvin, K. L., Price, C. E., Eds.; Academic Press: London, U.K., 1982; pp 139−166.

(6) Katagi, T. Photodegradation of pesticides on plant and soil surfaces. *Rev. Environ. Contam.Toxicol.* **2004**, *182*, 1−195.

(7) Meier, U. Leaf vegetable (forming heads). In *Growth Stages of Mono- And Dicotyledonous Plants*; BBCH Monograph; Federal Biological Research Centre for Agriculture and Forestry: Berlin, Germany, 2001; pp 120−123.

(8) Nambu, K.; Ohkawa, H.; Miyamoto, J. Metabolic fate of phenothrin in plants and soils. *J. Pestic. Sci.* **1980**, *5*, 177−197.

(9) Mikami, N.; Baba, Y.; Katagi, T.; Miyamoto, J. Metabolism of the synthetic pyrethroid fenpropathrin in plants. *J. Agric. Food Chem.* **1985**, *33*, 980−987.

(10) Cole, L. M.; Casida, J. E.; Ruzo, L. O. Comparative degradation of the pyrethroids toralomethrin, tralocythrin, deltamethrin, and cypermethrin on cotton and bean foliage. *J. Agric. Food Chem.* **1982**, *30*, 916−920.

(11) Gaughan, L. C.; Casida, J. E. Degradation of *trans*- and *cis*-permethrin on cotton and bean plants. *J. Agric. Food Chem.* **1978**, *26*, 525−528.

(12) Agency for Toxic Substances and Disease Registry. Toxicological profile for pyrethrin and pyrethroids, U.S. Department of Health and Human Services, September 2003; available at http://www.atsdr.cdc.gov/ToxProfiles/tp155.pdf.

(13) Laskowski, D. A. Physical and chemical properties of pyrethroids. *Rev. Envion. Contam. Toxicol.* **2002**, *174*, 49−170.

(14) Ruzo, L. O.; Kimmel, E. C.; Casida, J. E. Ozonides and epoxides from ozonization of pyrethroids. *J. Agric. Food Chem.* **1986**, *34*, 937−940.

(15) Pryor, A. W.; Giamalva, D.; Church, D. F. Kinetics of ozonation. 3. Substituent effects on the rates of reaction of alkenes. *J. Am. Chem. Soc.* **1985**, *107*, 2793−2797.

(16) Griesbaum, K.; Quinkert, R. O.; McCullough, K. J. C−C bond formation at ozonide rings by substitution of chlorinated ozonides. *Eur. J. Org. Chem.* **2004**, *17*, 3657−3662.

(17) Bauld, N. L.; Thompson, J. A.; Hudson, C. E.; Bailey, P. S. Stereospecificity in ozonide and cross-ozonide formation. *J. Am. Chem. Soc.* **1968**, *90*, 1822−1830.

(18) Ponec, R.; Yuzhakov, G.; Hass, Y.; Samuni, U. Theoretical analysis of the stereoselectivity in the ozonolysis of olefins. Evidence for a modified criegee mechanism. *J. Org. Chem.* **1997**, *62*, 2757−2762.

(19) Bailey, P. S.; Ferrell, T. M. Mechanism of ozonolysis. A more flexible stereochemical concept. *J. Am. Chem. Soc.* **1978**, *100*, 899−905.

(20) Murray, R. W.; Youssefyeh, R. D.; Story, P. R. Ozonolysis. Steric and stereochemical effects in the olefin. *J. Am. Chem. Soc.* **1967**, *89*, 2429−2434.

(21) Criegee, R. Mechanism of ozonolysis. *Angew. Chem. Int. Ed.* **1975**, *14*, 745−752.

(22) Geletneky, C.; Berger, S. The mechanism of ozonolysis revised by ^{17}O-NMR spectroscopy. *Eur. J. Org. Chem.* **1998**, *8*, 1625−1627.

(23) Zaikov, G.; Rakovsky, S. *Ozonation of Organic and Polymer Compounds*; Smithers Rapra: Shropshire, U.K., 2009; Chapter 3, pp 179−218.

(24) Perry, S. C.; Charman, A. S.; Prankerd, J. R.; Chiu, K. F. Chemical kinetics and aqueous degradation pathways of a new class of ozonide antimalarials. *J. Pharm. Sci.* **2006**, *95*, 737−747.

(25) Pryor, A. W. Can vitamin E protect humans against the pathological effects of ozone in smog? *Am. J. Clin. Nutr.* **1991**, *53*, 702−722.

(26) Guengerich, F. P. Cytochrome p450 oxidations in the generation of reactive electrophiles: epoxidation and related reactions. *Arch. Biophys. Biochem.* **2003**, *409*, 59−71.

(27) Hayashi, O.; Kameshiro, M.; Satoh, K. Intrinsic bioavailability of ^{14}C-heptachlor to several plant species. *J. Pestic. Sci.* **2010**, *35*, 107−113.

(28) Vaz, A. D. N.; McGinnity, D. F.; Coon, M. J. Epoxidation of olefins by cytochrome P450: evidence from site-specific mutagenesis for hydroperoxo-iron as an electrophilic oxidant. *Proc. Natl. Acad. Sci. U.S.A.* **1998**, *95*, 3555−3560.

(29) Sauveplane, V.; Kandel, S.; Kastner, P.; Ehlting, J.; Compagnon, V.; Wrek, R. D.; Pinot, F. *Arabidopsis thaliana* CYP77A4 is the first cytochrome P450 able to catalyze the epoxidation of free fatty acids in plants. *FEBS J.* **2009**, *276*, 719−735.

(30) Kaneko, H. Pyrethroid chemistry and metabolism. In *Hayes' Handbook of Pesticide Toxicology*, 3rd ed.; Krieger, R., Ed.; Elsevier: Amsterdam, The Netherlands, 2010; Chapter 76, pp 1635−1663.

(31) Ando, T.; Toia, R. F.; Casida, J. E. Epoxy and hydroxy derivatives of (*S*)-bioallethrin and pyrethrins I and II: synthesis and metabolism. *J. Agric. Food Chem.* **1991**, *39*, 606−611.
(32) Ando, T.; Jacobsen, N. E.; Toia, R. F.; Casida., J. E. Epoxychrysanthemates: two-dimensional NMR analyses and stereochemical assignments. *J. Agric. Food Chem.* **1991**, *39*, 600−605.
(33) Class, T. J.; Ando, T.; Casida, J. E. Pyrethroid metabolism: microsomal oxidase metabolism of (*S*)-bioallethrin and the six natural pyrethrins. *J. Agric. Food Chem.* **1990**, *38*, 529−537.
(34) Blee, E.; Schuber, F. Regio- and enantioselectivity of soybean fatty acid epoxide hydrolsase. *J. Biol. Chem.* **1992**, *286*, 5197−5203.